# Statistical Subspace-Based Damage Detection and Jerk Energy Acceleration for Robust Structural Health Monitoring

Khizar Hayat [1], Saqib Mehboob [1], Qadir Bux alias Imran Latif Qureshi [2,*], Afsar Ali [1], Matiullah [1], Diyar Khan [3,*] and Muhammad Altaf [1]

[1] Department of Civil Engineering, University of Engineering and Technology, Taxila 47080, Pakistan; khizar.hayat@students.uettaxila.edu.pk (K.H.); syed.saqib@uettaxila.edu.pk (S.M.); afsar.ali@students.uettaxila.edu.pk (A.A.); matiullah@students.uettaxila.edu.pk (M.); dm.altaf@uettaxila.edu.pk (M.A.)

[2] Department of Civil and Environmental Engineering, College of Engineering and Architecture, University of Nizwa, Birkat-al-Mouz, Nizwa 616, Oman

[3] Department of Road Transport, Faculty of Transport and Aviation Engineering, Silesian University of Technology, 40-019 Katowice, Poland

\* Correspondence: qadir.omran@unizwa.edu.om (Q.B.a.I.L.Q.); diyar.khan@polsl.pl (D.K.)

**Abstract:** This paper introduces a multistep damage identification process that is both straightforward and useful for identifying damage in buildings with regular plan geometries. The algorithm proposed in this study combines the utilization of a multi-damage sensitivity feature and MATLAB programming, providing a comprehensive approach for the structural health monitoring (SHM) of different structures through vibration analysis. The system utilizes accelerometers attached to the structure to capture data, which is then subjected to a classical statistical subspace-based damage detection test. This test focuses on monitoring changes in the data by analyzing modal parameters and statistically comparing them to the structure's baseline behavior. By detecting deviations from the expected behavior, the algorithm identifies potential damage in the structure. Additionally, the algorithm includes a step to localize damage at the story level, relying on the jerk energy of acceleration. To demonstrate its effectiveness, the algorithm was applied to a steel shear frame model in laboratory tests. The model utilized in this study comprised a total height of 900 mm and incorporated three lumped masses. The investigation encompassed a range of scenarios involving both single and multiple damages, and the algorithm proposed in this research demonstrated the successful detection of the induced damages. The results indicate that the proposed system is an effective solution for monitoring building structure condition and detecting damage.

**Keywords:** statistical tests; damage detection; damage localization; vibrational analysis; structural health monitoring

## 1. Introduction

Modern economies are highly reliant on critical civil engineering structures, including bridges, high-rise buildings, and industrial facilities. However, a significant challenge arises as a considerable portion of this infrastructure, along with the associated goods, in developed nations is approaching the conclusion of its initial design life cycle. Numerous fatalities and significant financial losses have resulted from catastrophic incidents caused by structural deterioration, failure, or the accumulation of damage. To reduce these expenses, governments allocate substantial annual budgets toward the maintenance and refurbishment of existing facilities [1].

In recent decades, the monitoring of civil structures' integrity has emerged as a crucial domain of research, encompassing various interconnected fields such as automatic control, bridge aging, earthquake resilience, and the preservation of historic and heritage structures. Vibration-based structural health monitoring (SHM) has been established as a fundamental

concept within this realm, predicated on the premise that damage significantly impacts the dynamic characteristics of a structure [2]. Within the context of structural health monitoring (SHM), the identification of damage stands as a pivotal challenge that must be addressed before advancing toward more advanced stages of damage diagnosis, including damage localization, quantification, and lifetime prediction [3]. The fundamental concept revolves around the notion that damage-induced alterations in the stiffness, mass, or damping characteristics of a structure inevitably lead to changes in its dynamic properties. Consequently, by leveraging the observed vibration data of the system, these dynamic properties can be assessed. Output-only techniques, specifically those grounded in ambient excitation principles, hold particular appeal in this context. Such techniques enable the evaluation of dynamic properties within customary operational conditions, obviating the requirement for human intervention. The evaluation of changes in damage-sensitive features derived from measurements in the system's current test state (possibly damaged or unhealthy) and its (undamaged or healthy) reference state can then be used to perform data-driven damage detection [4,5]. Because the features utilize ambient vibration data, statistical variability may have an impact on them. As a result, it is critical to consider the statistical properties of the elements when evaluating them in order to determine whether a change is significant: that is, whether there is damage or not.

Damage detection techniques can be classified into two major categories: model-based and model-free methods. Model-based approaches typically rely on the availability of a precise finite element (FE) model, which can demand substantial computational resources [6]. One method in the model updating category is the finite element model updating technique. It is extremely useful for monitoring the structural health of less complex structures. While it is highly challenging to update complex structures using finite element updating because it requires extensive computational and analytical skills and practice, because model-free methods of damage detection do not require model updating, they provide computational simplicity. These techniques employ digital signal processing to analyze variations in damage-related characteristics extracted from dynamic responses or their spectra. These techniques can be classified into two domains: time domain methods and frequency domain methods [7,8].

This study examines and explores the statistical subspace-based damage detection method described in the referenced paper [9–11]. This approach entails comparing data obtained during the potentially damaged state with a data-driven model derived from the undamaged or reference state. It avoids the need for the direct estimation of modal parameters in the potentially damaged states by utilizing a statistical subspace-based residual method. Additionally, a chi-square test, derived from the residual method, is employed for further analysis. The advantages include a fully automated procedure for locating the test value in a potentially damaged state. To ascertain the presence of damage, the calculated chi-square test value is compared against a predefined threshold. The chi-square value at the reference state is used as the threshold.

Energy shocks are used as indices in the majority of the most advanced damage detection techniques for damage localization. Energy distributions have been used to detect structural changes and damage [12]. Other energy-based techniques, such as the frequency response curvature function (FRF) [13], have made significant progress. Energy-based techniques can be effectively employed for the detection, measurement, and localization of structural damage. However, it is crucial to recognize that these techniques necessitate distinct frameworks tailored to the specific characteristics of each individual structure.

Thus, a basic and simple energy-based method that might be practical in terms of deployment on almost all kinds of structures is needed. Many existing algorithms [14–16] have the disadvantage of being susceptible to changes in the unidentified ambient vibration, which may result in false alarms. Moreover, the technique's viability under varying excitation [17–19] is also a challenging aspect of the SHM systems. Thus, to contribute to the area of SHM by reducing the real-field challenges associated with the deployment of any SHM system on real buildings, an improved damage index known as "jerk energy of acceleration" is

proposed for detecting damage in real time. The proposed method directly processes the measured vibrational data using the time-domain analysis approach. The objective of this research is to validate and demonstrate the proposed novel methodology using a test case study on a laboratory frame model at various excitation and damage levels. The point-wise idea and contribution of this modified and improved novel approach to structural health monitoring (SHM) for story level damage detection and localization is presented in Table 1.

**Table 1.** Novel approach using acceleration energy for damage identification.

| Description | Existing Methods | Novelty for Damage Identification |
|---|---|---|
| Damage detection methods employed energy-based indices. | Energy-based damage detection with information of loading and same load amplitude for each test case. | Curvature of acceleration jerk energy waveform ACJEW—avoid variation due to inputs amplitude. |
| Modal parameter extraction for damage detection and quantification. | Natural frequency may vary due to temperature and humidity effects. | Statistical subspace-based damage detection method for damage detection phase. |

This research paper is structured as follows: Section 2 introduces the fundamental concepts underlying the adopted damage detection approach, while Section 3 outlines the essential principles of the methods employed for damage localization. Section 4 presents a damage detection and localization algorithm on a simulated steel shear frame. Sections 5 and 6 present the results of damage detection and localization and conclude with closing remarks, respectively.

## 2. Statistical Subspace-Based Damage Detection Method

The behavior of the structure can be effectively characterized by a linear time-varying dynamic system as presented in Equation (1).

$$m\ddot{x}(t) + c\dot{x}(t) + kx(t) = v(t) \tag{1}$$

where $t$ represents time, $k$, $m$ and $c$ are the stiffness, mass, and dampness matrices, respectively, and $x$ accumulates the distance or displacement of the structure's DOF (degrees of freedom). White noise is utilized to model the external, unmeasured force $v(t)$.

Let us use accelerometers, for example, through critiquing system 1 at r coordinates. The discrete-time state-space model is obtained by discretizing system 1 over time and converting it into a first-order system.

$$\begin{cases} x_{k+1} = Ax_k + v_k \\ y_k = Cx_k + w_k \end{cases} \tag{2}$$

with the $x_k \in n$, the yield $y_k \in r$, the transition matrix $A \in n \times n$ and the analysis matrix $C \in n \times n$, where r is the number of transducers and $n$ is the order of the system. The vibrations, a measured Gaussian white noise sequence $v_k$, have zero mean and constant covariance during a measured series of Gaussian white noise, where $Q : E(V_k V^T_{k^j}) \overset{def}{=} Q\delta(k - k^j)$ represents the measurement noise and the expectation operator, respectively.

### 2.1. Properties from Subspace-Based System Identification

A residual function is built for the damage detection approach and is related to characteristics via subspace-based system identification driven by covariance. Let $G = E(x_k + 1y^T_k)$ be the difference between outputs and states and suppose $R_i = E(y_k y^T_{k-i}) = CA^{i-1}G$ is the theoretical covariance and

$$H_{p+1,q} \stackrel{def}{=} \begin{bmatrix} R_1 & R_2 & \dots & R_q \\ R_2 & R_3 & \dots & R_{q+1} \\ \vdots & \vdots & \ddots & \vdots \\ R_{p+1} & R_{p+2} & \dots & R_{p+q} \end{bmatrix} \stackrel{def}{=} Hank(R_i) \tag{3}$$

is the theoretical block Hankel matrix of class $(p+1)r \times qr$ where parameters $p$ and $q$ are chosen such that $min\{pr, qr\} \geq n$ with often $p+1 = q$. Matrix $H_{p+1,q}$ possesses the well-known factorization property.

$$H_{p+1,q} = O_{p+1}C_q \tag{4}$$

The matrices of observability and controllability

$$O_{p+1} = \begin{bmatrix} C \\ CA \\ \vdots \\ CA^p \end{bmatrix}, C_q = \begin{bmatrix} G\ AG \dots A^{q-1}G \end{bmatrix} \tag{5}$$

The matrices $C$ and $A$, as well as the modal parameters, might be retrieved from the obsessive-compulsive matrix $O_{p+1}$. Instead of using system identification, the fact is employed that damages cause changes in $A$ and $C$ and subsequently in $H_{p+1,q}$ through Equations (4) and (5). This fact will be directly tested in the statistical test.

*2.2. Damage Detection Test*

The parametric and non-parametric damage detection test is detailed in the paragraphs that follow. A reliable estimate of the Hankel matrix $H_{p+1,q}$ is generated from the employing measured data, empirical output covariances $(y_k)_{k=1,\dots,N}$

$$\hat{R}_i = \frac{1}{N}\sum_{k=1}^{N} y_k y^T_{k-i}, \hat{H}_{p+1,q} = \text{Hank}(\hat{R}_i) \tag{6}$$

Let $H^{ref}_{p+1,q}$ calculate the left null space of the Hankel Matrix in the reference state using single value decomposition (SVD).

$$\hat{H}^{ref}_{p+1,q} = [\hat{U}_1\ \hat{U}_0] \begin{bmatrix} \hat{\Delta}_1 & 0 \\ 0 & \hat{\Delta}_0 \end{bmatrix} \begin{bmatrix} V_1^T \\ V_0^T \end{bmatrix} \tag{7}$$

Here, $S = \hat{U}_0$ where $\hat{\Delta}_1$ is of size $n \times n$ and where $\hat{\Delta}_0 \approx 0$. The characteristic property of the reference state then will be:

$$S^T \hat{H}_{p+1,q} \approx 0 \tag{8}$$

While in the damaged state, the product deviates from 0. The residual vector $\zeta$ determines whether the measured data match the reference state.

$$\zeta = \sqrt{N}\ vec\left(S^T \hat{H}_{p+1,q}\right) \tag{9}$$

Then, $\chi^2$ is used to determine whether or not this residual is different from zero.

$$\chi^2_\zeta = \zeta^T \Sigma_\zeta^{-1} \zeta \tag{10}$$

The number of data from the undamaged state is used to construct the empirical residual covariance $\Sigma_\zeta = \text{cov}(\zeta)$. The $\chi^2$ test value is compared to the data from the undamaged state to determine if damage is there or not. The threshold can also be generated

from test values on various data from the undamaged state, where the residual covariance is obtained from different numerical data from data sets.

$$\zeta_\zeta^2 = \zeta^T \sum_\zeta^{-1} \zeta \tag{11}$$

*2.3. Robust Damage Detection Test under Changing Excitation*

Even if there is no structural change, a change in the cross-covariance G between the states and outputs and consequently in the Hankel matrix estimate $\hat{H}_{p+1,q}^{ref}$ are caused by a change in the covariance Q of the unmeasured vibrations $V_k$ of the system. As a result, variations in the ambient excitation can influence the residual and the corresponding test value 2, potentially leading to false alarms.

These factors prompted the development of a robust damage detection test. Based on the logic that the matrix $\hat{H}_{p+1,q}^{ref}$ and the matrix of its main vectors $\hat{U}_1$ represents the null space S, the reference state may be represented as $S^T \hat{U}_1 \approx 0$.

The orthonormal columns of matrix $\hat{U}_1$ allow it to be known as irrespective of the vibrational properties, in contrast to the Hankel matrix $\hat{H}_{p+1,q}^{ref}$, which is related to the ambient vibration data properties. A unique SVD is used to define $\hat{U}_1$ to ensure that the modal basis does not change (for example, by requiring the initial data in each entry in columns to be greater than zero).

$$\zeta = \sqrt{N}\, vec(S^T \hat{U}_1) \tag{12}$$

The $\chi^2$ is used to determine whether or not this residual is either less than, greater than, or equal to zero.

**3. Damage Localization Based on Jerk Energy of Acceleration Response**

In physics, jerk or jolt is the time rate of change of acceleration, and as such, the second derivative of velocity, or the third derivative of displacement. It is a vector quantity (having both magnitude and direction). Jerk is most commonly denoted by the symbol j and expressed in m/s$^3$ [20,21].

$$Jerk = j(t) = \frac{da(t)}{dt} = \frac{d^2v(t)}{dt^2} = \frac{d^3x(t)}{dt^3} \tag{13}$$

Let $a_1, a_2, a_3, \ldots\ldots, a_n$ represent the sampled points of the acceleration data of a signal; then, the jerk at a particular time $x$ is given by Equation (14).

$$j_x = \frac{a_{x+1} - a_x}{\Delta t} \tag{14}$$

where $\Delta t$ is the sampling time interval between two data points. The Gibbs–Appell equation [22,23] gives the acceleration energy associated with the signal $a$.

$$E = \frac{1}{2}\sum_{i=1}^{n} m_i a_i^2 \tag{15}$$

where $m_i$ is the mass, and $a_i$ is the acceleration of node $i$. By analogy, the jerk energy at node $i$ is defined as:

$$Jerk\ Energy = JE_i = \frac{1}{2}\sum_{x=1}^{n-1} m_i j_x^2 \tag{16}$$

When considering a signal's power, the higher amplitude information is emphasized, while the lower level is de-emphasized. The natural logarithm of the sum of the squares of the sampled average jerk at node $i$ over the entire time history is defined as follows [24,25]:

$$JE_i = \log \sum_{x=1}^{N-1} \left(j_x^i\right)^2 = \log \sum_{x=1}^{N-1} \left(\frac{a_{x+1} - a_x}{\Delta t}\right)^2 \tag{17}$$

where $i$ denotes the respective node number (story level where acceleration is recorded), $x$ denotes the respective number of acceleration data points at a particular time, $\Delta t$ denotes the sampling time interval between two data points, and log represents the natural logarithm. The jerk energy waveform (JEW) is computed at every node through connecting jerk energy values at every specified node. Then, the "curvature" of JEW at every specified node can be computed similarly by Equation (18).

$$C_i = \frac{JE_{i-1} - 2JE_i + JE_{i+1}}{h^2} \tag{18}$$

where $C_i$ represents the curvature of the jerk energy waveform at node is $i$, $JE_i$ is the jerk energy computed at node $i$, and $h$ represent the distance between two adjacent nodes. If the node number from the 1st to last story is represented by $1, 2, \ldots\ldots, n$, then the sequence of node numbering can be represented by a clockwise closed loop, as shown in Figure 1 (taking $i = 3$ in this case).
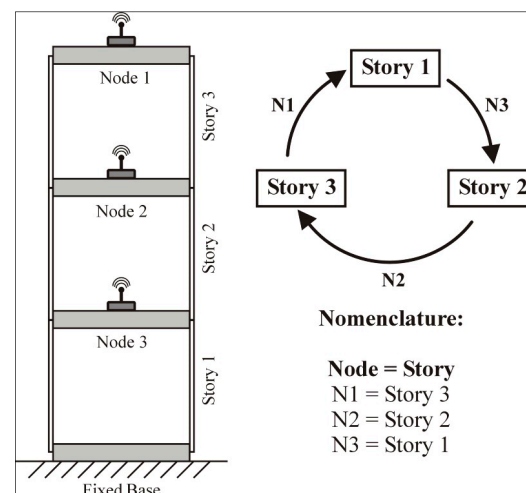


**Figure 1.** Clockwise closed loop of measured nodes.

Therefore, the curvature of the 1st and 3rd (last) node are computed as $C_1 = \frac{JE_i - 2JE_1 + JE_2}{h^2}$ and $C_i = \frac{JE_{i-1} - 2JE_i + JE_1}{h^2}$, respectively; thus, the curvature of JEW can be computed at all nodes including the 1st and last node. The curvature difference of JEW at a specified node is computed by subtracting the JEW curvature after damage from the JEW curvature before damage, as given by Equation (18).

$$\left(C_\Delta^i\right)_{rs} = \left(C_r^i\right)_{before} - \left(C_s^i\right)_{after} \tag{19}$$

where, $r$ and $s$ refer to responses recorded before damage and after damage, respectively. $\left(C_r^i\right)_{before}$ represents the JEW curvature for the $r^{th}$ response and $\left(C_s^i\right)_{after}$ represents the JEW curvature for the $s^{th}$ response at node $i$.

### 3.1. Damage Localization—Stage I

To determine the damaged story, first employ a damage index ($DI_1$) based on the mean normalized curvature difference of JEW $\left(C_\Delta^i\right)_{rs}$. Once the JEW curvature difference values are known, the damaged story can be located as shown below:

$$\left(C_\Delta^i\right)_{rs}^* = \left(C_\Delta^i\right)_{rs} / \max\left(C_\Delta^i\right)_{rs} \tag{20}$$

The mean normalized curvature difference is taken at each node, and this mean value gives the first damage index $\mu_i$ as follows:

$$(DI_1)_i = \mu_i = \frac{1}{RS}\sum_{r=1}^{r}\sum_{s=1}^{s}\left(C_\Delta^i\right)_{rs}^* \tag{21}$$

As a rule of thumb, *RS* is taken to be 10 or greater, but generally, *RS* is taken to be 20. A threshold value is defined while using only data of the undamaged structure; a detailed procedure is given in Section 3.2. A story having a mean value greater than or equal to the threshold value ($\delta$) is considered as damaged.

### 3.2. Damage Localization—Stage II

The Curvature Difference Probability of Jerk Energy Waveform (CDPJEW) method relies on the utilization of the Heaviside step function. In this second stage of localization, the following steps should be performed after the determination of the normalized curvature difference $\left(C_\Delta^i\right)_{rs}^*$ at each node to localize the damage. The normalized curvature difference values equal to and greater than $\delta$ are determined, i.e., if the normalized value of the curvature difference at the given node $i$ is equal to or greater than $\delta$, $\Gamma_{rs}^i$ is 1; otherwise, $\Gamma_{rs}^i$ takes the value of zero.

$$\Gamma_{rs}^i = H\left\{\left(C_\Delta^i\right)_{rs}^*\right\} \tag{22}$$

where *H* represents the Heaviside step function. The mean of the $\Gamma_{rs}^i$ is taken as the second damage index $DI_2$, while the second damage index is also known as damage probability and is given by Equation (19).

$$(DI_2)_i = \frac{1}{RS}\sum_{r=1}^{R}\sum_{s=1}^{S}\Gamma_{rs}^i \tag{23}$$

A threshold value $\rho$ is selected for the damage probability damage index. The node representing the story is considered as damaged if the damage probability is greater than the probability threshold value at a specified node.

### 3.3. Rule of Localization

Generalizing the rule (see Figure 1), if the *i*th node/story resulting values of the $DI_1$ and $DI_2$ are greater than threshold values, it means the element/story one ahead of the location where index value exceeds the threshold will represent the actual damage location in the clockwise closed loop model.

## 4. Algorithm Development and Implementation

The precise execution of the damage identification process, which involves detecting the presence of damage and accurately localizing it, is of utmost importance in the domain of structural health monitoring (SHM) for civil engineering structures. Despite the fact that the techniques described such as frequency domain decomposition and Modal Assurance Criterion (MAC) have some limitations on practical grounds, still, they are found to be very complementary and effective up to certain levels [25]. When considering the SHM levels, it would be possible to precisely detect and localize damage by applying the chi-square test and jerk energy-based identification in a particular order. Figure 2 shows the suggested damage detection and localization algorithm.
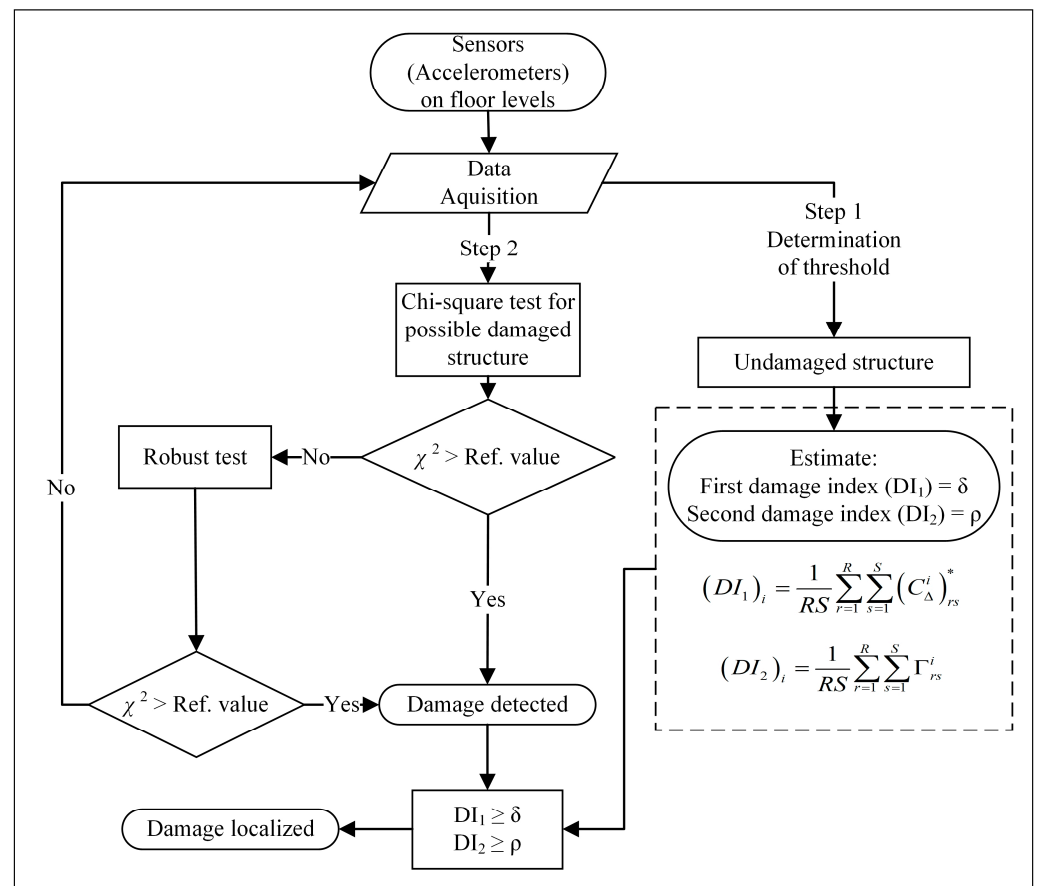
**Figure 2.** Damage detection and localization algorithm.

This algorithm has two levels: detection and localization. The chi-square test and reliable test procedures are part of the detection level. These statistical tests are applied to the processing of the ambient vibration data at reference and damage states. The chi-square test is initially used due to its simplicity and sensitivity. The detection of damage occurs when the test value in the damaged state exceeds the corresponding value in the reference state and vice versa. The chi-square test makes determining the threshold value simple; in fact, the test value at the reference state serves as the threshold value. White noise and other errors can make it difficult to find damage with straightforward tests. The left null space vector was then used in a robust test that avoids white noise. The jerk energy of the acceleration responses from all story levels is used during the localization stage. In general, the localization outcomes are precise.

## 5. Experimental Validation

The algorithm proposed in this study was validated using a steel shear frame model structure. Figure 3 shows the proposed structure and experimental setup. The model utilized in this study consisted of an elastic steel material, featuring a total height of 900 mm and incorporating three lumped masses. The vibration analysis was performed along a single axis of the coordinate system. To facilitate data collection, accelerometers were strategically installed on each floor of the model. The columns were characterized by cross-sectional dimensions of 28.43 × 2.1 mm in the undamaged case. At the beam–column joint level, the horizontal floor beams, measuring 274 mm in length, were securely fastened together, utilizing a tightly screwed connection. The cross-section of the floor beams was 25.33 × 25.33 mm. The mass of each floor beam is approximately 1.35 kg. The time vs. acceleration response of the model building is presented in Figure 3, representing the

responses at locations 1, 2 and 3 as indicated. The time is measured in seconds and *y*-axis acceleration is measured in g units.
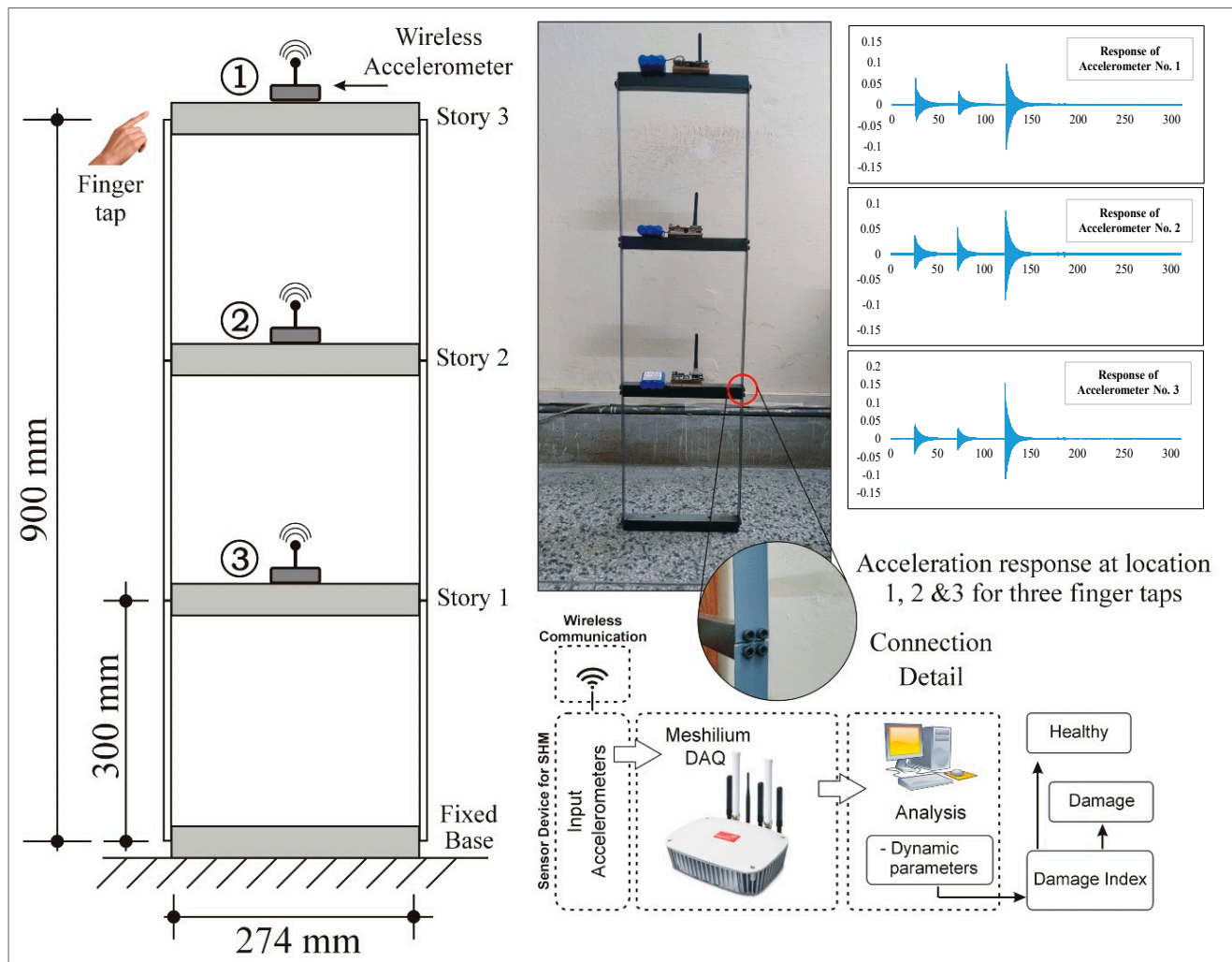


**Figure 3.** Experimental setup of an elastic model of shear frame and structural response of UD case for ambient vibration response.

Subsequently, various damage scenarios have been introduced in the research community to replicate real-world conditions, with some widely accepted approaches. These methods encompass reducing the cross-sectional area of the member to lower the floor stiffness, substituting the member with a different material, introducing saw-cuts or fractures in the member, and loosening connection bolts, among other techniques. In this study, the simulated degradation of floor stiffness, which is a common type of building damage, was implemented by replacing the columns at different story levels with members possessing a smaller cross-section (28.43 × 0.98 mm). This methodology effectively represents the condition of structural health monitoring (SHM) for civil structures, as it emulates damage commonly encountered in practical scenarios. However, it should be emphasized that the selection of steel bars to represent the columns in the physical model was based on their local availability and suitability. In the following section (Section 5.1), an in-depth exploration and discussion of different damage scenarios utilizing the available cross-sectional sizes were presented.

*5.1. Damage Scenarios*

The current investigation examines six specific damage cases (DCs) as detailed in Table 1. These cases involve deliberately reducing the column thickness, resulting in a decrease in the moment of inertia of the columns at various story levels, thereby introducing damage. Both single damage (SD) and multiple damage (MD) scenarios were considered, where columns at specific story levels were replaced with members featuring reduced cross-sections. To maintain consistency in the structural connections pre- and post-damage, the connecting bolts were securely refastened subsequent to each member replacement.

In DC1-SD, DC2-SD, and DC3-SD, the columns at the designated story level are replaced with members possessing reduced cross-sections, while the columns in all other stories maintain a bending direction moment of inertia of 21.94 $mm^4$. On the other hand, DC4-MD, DC5-MD, and DC6-MD correspond to cases involving multiple damages, as specified in Table 2. Empirical observations have demonstrated that deliberately induced damage at a designated story level, irrespective of whether it affects a single or multiple stories, results in substantial modifications in the structural frequencies.

**Table 2.** Details of different damage scenarios for steel frame model.

| Cases | Description |
|---|---|
| Undamaged (UD) | All columns of same cross-section at each story level |
| DC1-SD | Columns of story-1 are replaced with reduced cross-sectioned members |
| DC2-SD | Columns of story-2 are replaced with reduced cross-sectioned members |
| DC3-SD | Columns of story-3 are replaced with reduced cross-sectioned members |
| DC4-MD | Columns of story-1 and story-2 are replaced with reduced cross-sectioned members |
| DC5-MD | Columns of story-2 and story-3 are replaced with reduced cross-sectioned members |
| DC6-MD | Columns of story-1 and story-3 are replaced with reduced cross-sectioned members |

Note: Moment of inertia of each column in bending direction is 21.94 $mm^4$ and 2.09 $mm^4$ for undamaged and damaged demonstration, respectively.

## 6. Results

*6.1. Damage Detection*

6.1.1. Chi-Square Test

The results are classified as single-story or multi-story damage detection. At each level of excitation, all of the measured data sets, both in their "reference/undamaged" and "damaged" states, are tested. Figure 4a,b show the computed test values for the $\chi^2$ test as well as an empirical threshold calculated using the reference state's test values. The $\chi^2$ test responds strongly to various levels of excitement. No matter how much damage there is, lowering the level of excitation lowers the test value. While it is noteworthy that the test values exhibit a consistent increase in relation to the magnitude of damage across different levels of excitation, the rate of increase remains constant.

6.1.2. Robust Test

The outcomes of the robust test are presented in Figure 5a,b, providing clear evidence of enhanced robustness when considering diverse excitation properties. Despite the presence of minor variations in the test values within the reference state and states with minimal damage, their significance has significantly diminished. These variations in damage across individual stories appear to be independent of the level of excitation, thereby validating the robustness of the proposed test regardless of fluctuations in excitation level. Due to the robustness of the new test, even relatively minor damage can be clearly detected under varying excitations.
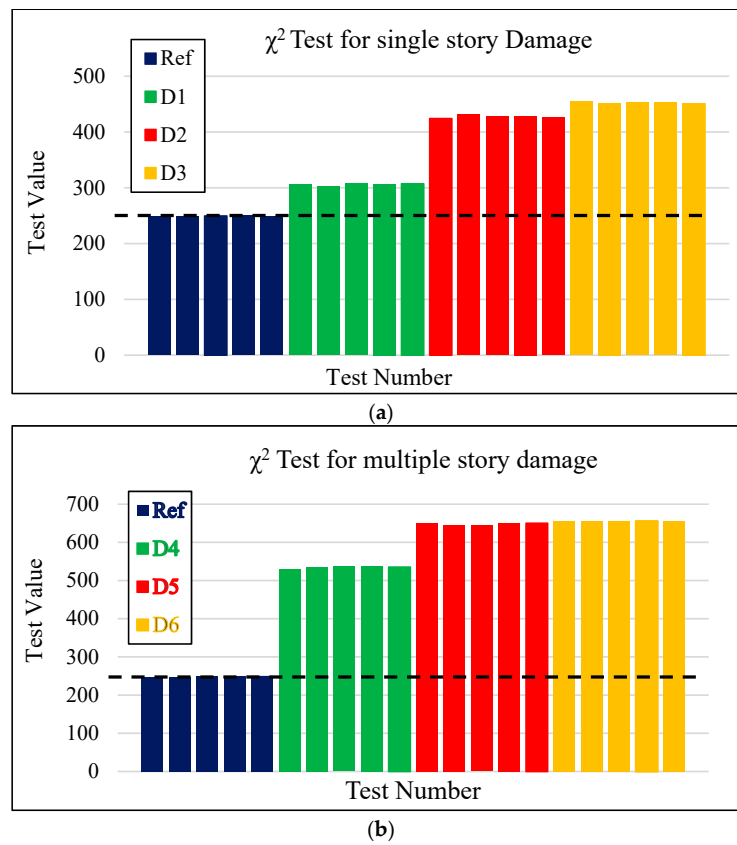
**Figure 4.** Chi-square test results: (**a**) Single-story damage; (**b**) Multi-stories damage.
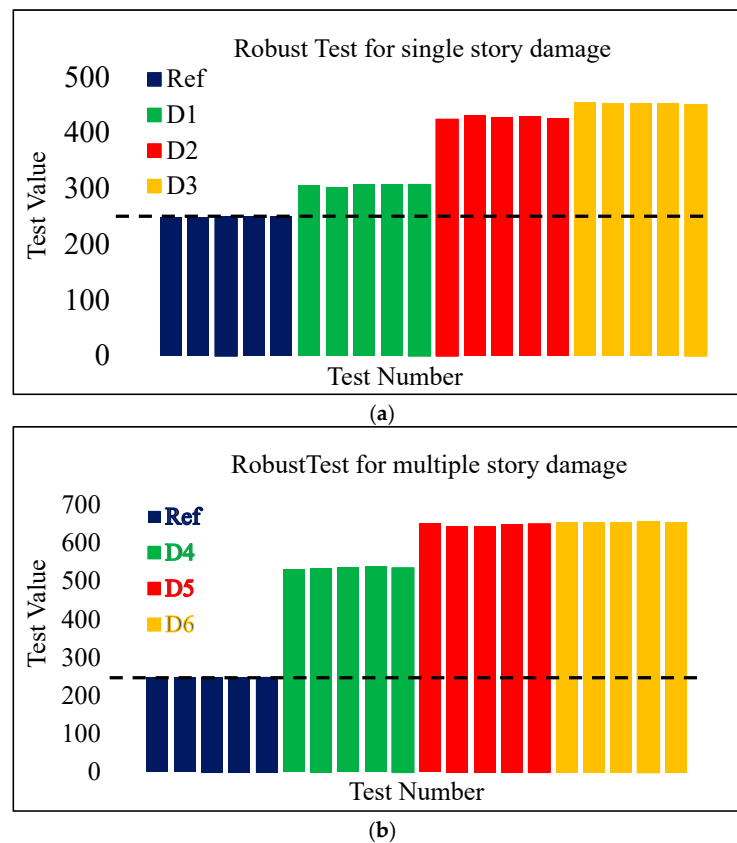


**Figure 5.** Robust test results: (**a**) Single-story damage; (**b**) Multi-stories damage.

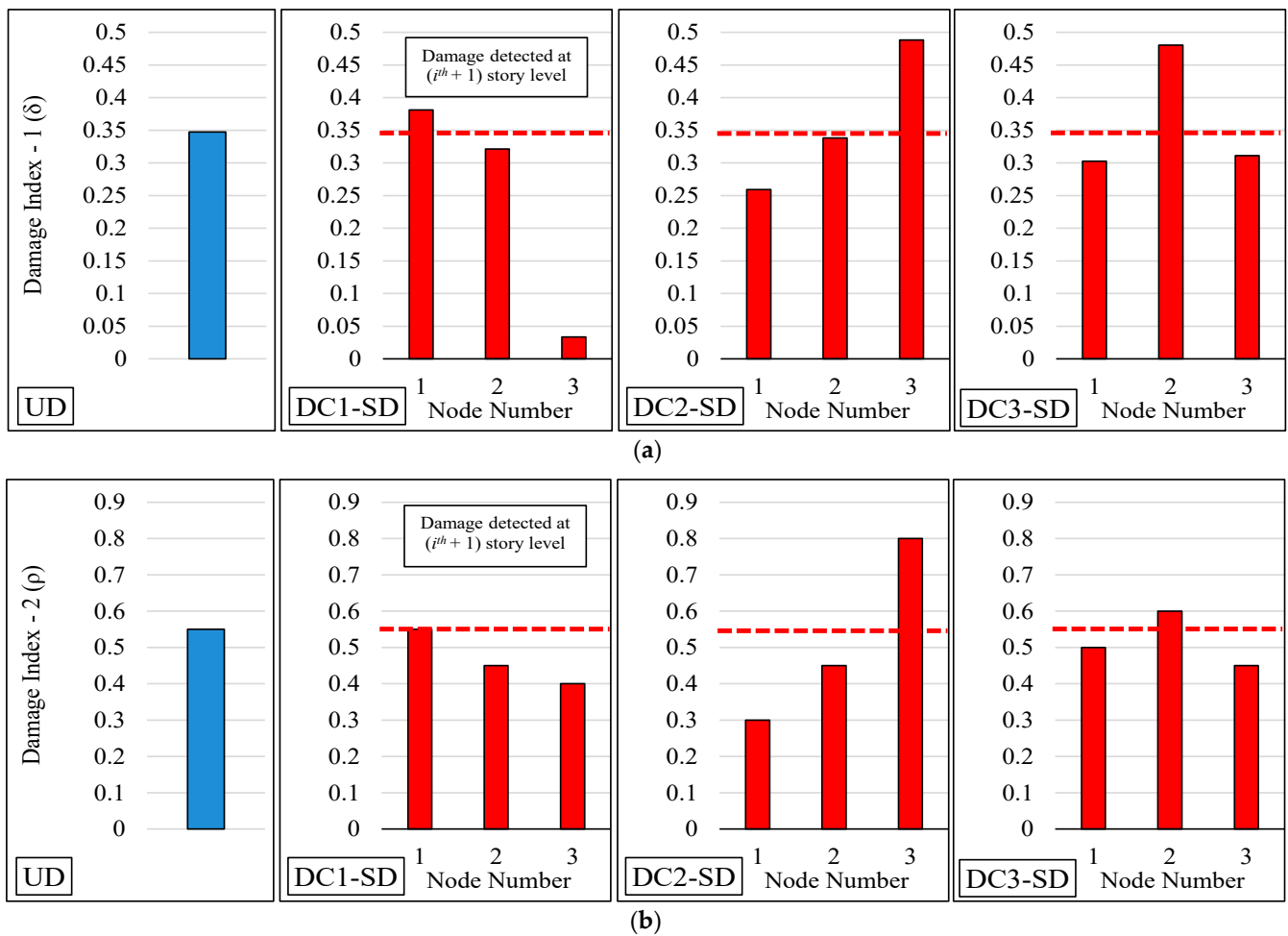*6.2. Damage Localization*

6.2.1. Threshold Determination

The mean normalized curvature of ACJEW and the normalized probability thresholds are calculated using intact structure accelerations. As a general rule, use the base signal from one set of five acceleration histories against free-vibration tests before repeating the process for a second set of four acceleration histories. To minimize the uncertainties caused by noise distortions, it should be noted that each set of acceleration signals should have more than five and four signals, respectively. It is also noteworthy that the final RS product selection must be greater than or equal to 10. As a result, multiple signals can be acquired, which can subsequently be utilized to identify undamaged cases. Next, a suitable threshold and probability threshold are established using these acceleration signals, representing Index-1 ($DI_1$) and Index-2 ($DI_2$), respectively. Figure 6 shows that for the three-story shear building model, the probability threshold is 0.55 (i.e., 55 percent), and the threshold is 0.3475 (say 0.35).
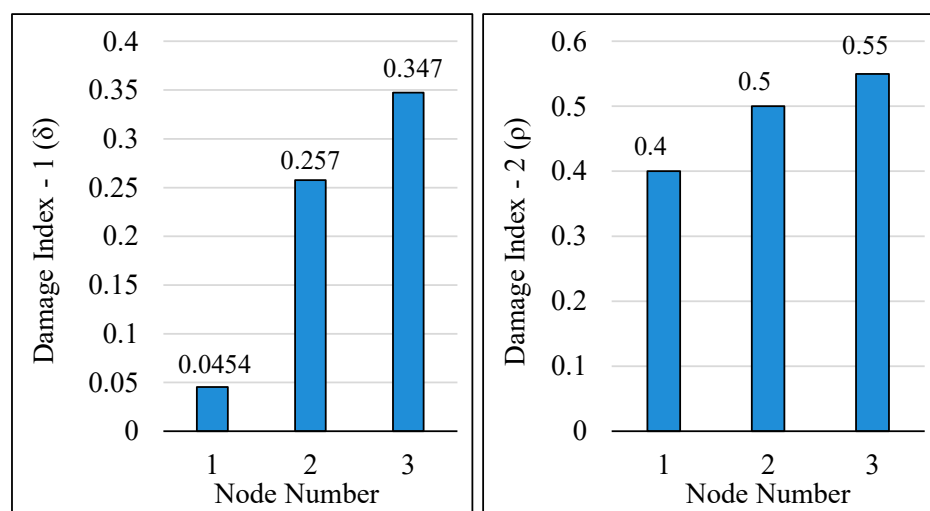


**Figure 6.** Threshold values results for damage indies, i.e., $DI_1$ and $DI_2$.

6.2.2. Single-Story Damage

Six experimental damage cases are considered in total, three of which represent single-story damage states and the other three of which cover three possible combinations of multiple damage states. The acceleration-based damage localization methods became active during the localization stage, and damages were localized. Figure 1 depicts the closed-loop model and associated nomenclature for matching the story number to the node number. Figure 7 shows that at node 1, which represents the acceleration response of story 3 (say the $i$th story), the values of the first and second damage localization indexes are 0.3813 and 0.55, respectively, representing damage at the first story (i.e., the $i$th + 1 story in the closed loop), and the values of the first and second damage localization indexes are 0.4882 and 0.8, respectively, representing damage at the second story. Similarly, in the third damage case, where the third story is actually damaged, the index values 0.4804 and 0.6 appeared at node 2, representing the acceleration response of story 2.

**Figure 7.** Damage localization based on JE methods for single damage cases. (**a**) Index-1: Mean normalized curvature of ACJEW. (**b**) Index-2: Probability damage index.

Thus, in the clockwise closed loop model, if the $i$th node resulting values of the $DI_1$ and $DI_2$ are equal to or greater than threshold values, the story one ahead of the respective $i$th node story will be detected as a damaged story (see Figure 1 for the closed loop model). With this rule in mind, finding the correct damage location for a single damage case is simple.

### 6.2.3. Multiple Stories Damage

According to Table 1, three potential multiple-story damage cases were evaluated using acceleration-based damage localization methods, and damages were localized. Figure 8 depicts the results for the shear frame model.

There is a point of note as observed in one of the multiple damage cases, i.e., DC4-MD. Damage localization based on the mean normalized curvature difference of ACJEW resulted in a partial detection, which means one damage story was identified while the other (2nd story) appeared undamaged using Index-1 (see Figure 8a). Figure 8b shows the localization of damages based on Index-2 and shows that every node (nodes 1 and 3) has a probability Index value greater or equal to 0.55 (55 percent); thus, all of the Index-2 results improve the damage localization process based on the probability of any story being damaged or undamaged, as presented herein based on the JE methods.

For the case DC6-MD, node number 1 and 2 having both index values more than threshold reflects that stories 1 and 3 are damaged, which are one ahead in the clockwise closed loop model with respect to their node number.
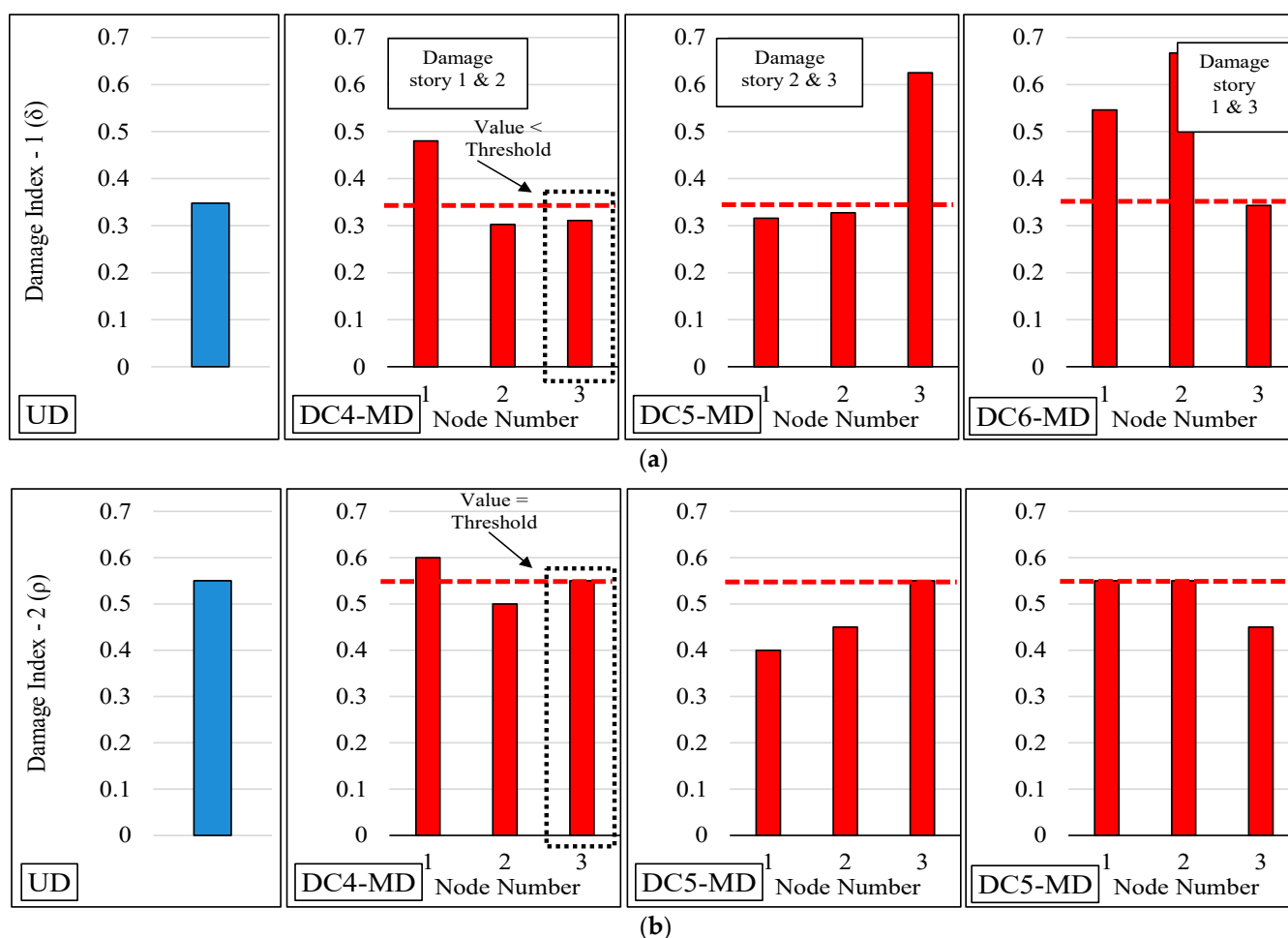
**Figure 8.** Damage localization based on ACJEW methods for multiple damage cases. (**a**) Index-1: Mean normalized curvature of ACJEW. (**b**) Index-2: Probability damage index.

## 7. Conclusions

This research work introduces an algorithm specifically designed for the detection and localization of damage in building frame structures. The primary objective was to develop a straightforward, rapid, and effective method for monitoring the health of civil engineering structures based on both global and local damage indices. The following are some final considerations:

1. With the help of the proposed algorithm, structural damage can be successfully identified and localized both in single- and multiple-story damage cases.
2. For damage to be detected, the chi-square test value in reference (the undamaged state) must be greater than or equal to the chi-square test value in the damaged state.
3. If a story is damaged in the clockwise closed loop model, the resulting values of the first and second damage localization indexes are always greater than the threshold values at a node preceding the node (damaged story). Keeping this rule in mind makes it easy to pinpoint the precise location of any damage.

This paper represents a significant phase of our ongoing research project. It has successfully achieved the set goals and purpose, shedding light on damage detection and localization as a part of SHM. It is hoped that the work presented here will serve as a useful contribution for future research into an economical, robust, and practical SHM system for real structures. However, it is important to note that this work is part of a larger effort, and future phases will delve further into investigation to examine the algorithm's response when applied to non-regular building structures with planar geometric irregularities. We acknowledge the need to thoroughly examine and discuss any limitations that may arise,

and we intend to address these in subsequent stages of the research. A large-scale SHM on a concrete building model is already built in this research work for further studies.

## References

1. Hassani, S.; Dackermann, U. A Systematic Review of Advanced Sensor Technologies for Non-Destructive Testing and Structural Health Monitoring. *Sensors* **2023**, *23*, 2204. [CrossRef] [PubMed]
2. Farrar, C.R.; Worden, K. An Introduction to Structural Health Monitoring. In *New Trends in Vibration Based Structural Health Monitoring*; Deraemaeker, A., Worden, K., Eds.; Springer: Vienna, Austria, 2010; pp. 1–17.
3. Tefera, B.; Zekaria, A.; Gebre, A. Challenges in applying vibration-based damage detection to highway bridge structures. *Asian J. Civ. Eng.* **2023**, *24*, 1875–1894. [CrossRef]
4. Chen, Y. Vibration-based structural damage localisation using time response correlation. *Nondestruct. Test. Eval.* **2023**, *38*, 112–129. [CrossRef]
5. Mehboob, S.; Khan, Q.U.Z.; Ahmad, S. Application of an Improved Damage Detection Method for Building Structures Based on Ambient Vibration Measurements. *Arab. J. Sci. Eng.* **2023**. [CrossRef]
6. Adewuyi, A.P.; Wu, Z. Vibration-based damage localization in flexural structures using normalized modal macrostrain techniques from limited measurements. *Comput.-Aided Civ. Infrastruct. Eng.* **2011**, *26*, 154–172. [CrossRef]
7. Qiao, L.; Esmaeily, A. An overview of signal-based damage detection methods. *Appl. Mech. Mater.* **2011**, *94*, 834–851.
8. Mehboob, S.; Khan, Q.U.Z.; Ahmad, S. Numerical study for evaluation of a vibration based damage index for effective damage detection. *Bull. Pol. Acad. Sci. Tech. Sci.* **2020**, *68*, 1443–1456.
9. Basseville, M.; Abdelghani, M.; Benveniste, A. Subspace-based fault detection algorithms for vibration monitoring. *Automatica* **2000**, *36*, 101–109. [CrossRef]
10. Basseville, M.; Mevel, L.; Goursat, M. Statistical model-based damage detection and localization: Subspace-based residuals and damage-to-noise sensitivity ratios. *J. Sound Vib.* **2004**, *275*, 769–794. [CrossRef]
11. Döhler, M.; Mevel, L. Subspace-based fault detection robust to changes in the noise covariances. *Automatica* **2013**, *49*, 2734–2743. [CrossRef]
12. Shi, Z.; Law, S.; Zhang, L.M. Structural damage detection from modal strain energy change. *J. Eng. Mech.* **2000**, *126*, 1216–1223. [CrossRef]
13. Reddy, D.M.; Swarnamani, S. Application of the FRF curvature energy damage detection method to plate like structures. *World J. Model. Simul.* **2012**, *8*, 147–153.
14. Wedel, F.; Marx, S. Application of machine learning methods on real bridge monitoring data. *Eng. Struct.* **2022**, *250*, 113365. [CrossRef]
15. Malekloo, A.; Ozer, E.; AlHamaydeh, M.; Girolami, M. Machine learning and structural health monitoring overview with emerging technology and high-dimensional data source highlights. *Struct. Health Monit.* **2022**, *21*, 1906–1955. [CrossRef]
16. Brethee, K.F.; Uwayed, A.N.; Alden Qwam, A.Y. A novel index for vibration-based damage detection technique in laminated composite plates under forced vibrations: Experimental study. *Struct. Health Monit.* **2023**. [CrossRef]
17. Döhler, M.; Mevel, L.; Hille, F. Subspace-based damage detection under changes in the ambient excitation statistics. *Mech. Syst. Signal Process.* **2014**, *45*, 207–224. [CrossRef]
18. Gres, S.; Ulriksen, M.D.; Döhler, M.; Johansen, R.J.; Andersen, P.; Damkilde, L.; Nielsen, S.A. Statistical methods for damage detection applied to civil structures. *Procedia Eng.* **2017**, *199*, 1919–1924. [CrossRef]
19. Yao, R.; Pakzad, S.N. Autoregressive statistical pattern recognition algorithms for damage detection in civil structures. *Mech. Syst. Signal Process.* **2012**, *31*, 355–368. [CrossRef]
20. Schot, S.H. Jerk: The time rate of change of acceleration. *Am. J. Phys.* **1978**, *46*, 1090–1094. [CrossRef]
21. Sandin, T. The jerk. *Phys. Teach.* **1990**, *28*, 36–40. [CrossRef]
22. Qiao, Y. Gibbs-Appell's equations of variable mass nonlinear nonholonomic mechanical systems. *Appl. Math. Mech.* **1990**, *11*, 973–983.

23. Vujanovic, B.D.; Atanackovic, T.M.; Atanacković, T.M. *An Introduction to Modern Variational Techniques in Mechanics and Engineering*; Springer Science & Business Media: Berlin/Heidelberg, Germany, 2004.

24. Bindi, D.; Petrovic, B.; Karapetrou, S.; Manakou, M.; Boxberger, T.; Raptakis, D.; Pitilakis, K.; Parolai, S. Seismic response of an 8-story RC-building from ambient vibration analysis. *Bull. Earthq. Eng.* **2015**, *13*, 2095–2120. [CrossRef]

25. Mehboob, S.; Zamana, Q.U. Vibration-based method for story-level damage detection of the reinforced concrete structure. *Comput. Concr. Int. J.* **2021**, *27*, 29–39.